Noise characteristics of correlated two-photon production via parametric down-conversion

Xianmei Meng

Department of Physics and Astronomy, University of New Mexico, Albuquerque, NM 87131

Tel: (505)-272-7922, Fax: (505)-272-7801, email: xmmeng@unm.edu

This paper gives a review of the phase and intensity quantum correlation between two photons in the process of optical parametric down-conversion (OPDC). Special emphasis is on the squeezed spectrum and squeezed intensity fluctuations in non-degenerate OPDC above threshold. Several experimental results of squeezed spectra and sub shot-noise intensity fluctuations are presented.

PACS number(s): 42.50.Lc , 42.50.Dv, 42.65.Ky

I. INTRODUCTION

Since the beginning of the theoretical research on squeezing in lasers, the problem of squeezed-state generation in two-photon systems has attracted much attention. This is because the two-photon pair generated through parametric down conversion are more efficient and well correlated than other processes, such as a three-body decay [1].

The correlated photon pairs produced in optical parametric down-conversion have many interesting properties. Theoretical and experimental studies have been published both on spontaneous parametric down-conversion (SPDC) and resonance parametric down-conversion, both degenerate and non-degenerate cases. Early experiments to study the spatial correlations were performed by Sergienko and co-workers [2]. Theoretical treatment of the transverse correlations in SPDC with emphasis on the geometry and physical optics properties of the two-photon amplitude was given by Rubin [3]. Recent experiments have illustrated some of the interesting effects of transverse correlations in image transfer [4,5] and on coincidence counting rate [6]. Theoretical and experimental studies of the polarization and frequency correlation of type-II SPDC have been published [7,8].

Squeezed states, which are generated by parametric down conversion process, are reported by many experiments, and noise reductions are observed in balanced homodyne detector [9-12]. The applications of squeezed states of light demonstrated in increasing signal-to-noise ratio of phase and amplitude measurement beyond the shot-noise limit [13]. Squeezed state generation of electromagnetic fields provides a means of reducing uncertainty in one electric field quadrature at the expense of a larger uncertainty in its conjugate partner, thus particular attention has been focused on squeezed states that are characterized by a phase-dependent redistribution of quantum fluctuations.

This paper is divided into four sections. In section II, a review of the theory of two-photon correlation above threshold is given. The emphasis is on how noise reduction in phase and amplitude can be achieved through the analysis of the quantum correlations of the two modes in non-degenerate parametric oscillation. In addition, it is interesting to notice that under the condition of minimum fluctuations, such quantum correlation between the signal and idler modes correspond to those of Einstein-Podolsky-Rosen (EPR). In section III, some experimental results of squeezed spectra and squeezed amplitude based on two-photon parametric down conversion are presented. Finally, in section IV we summarize.

II. THEORY OF TWO-PHOTON CORRELATION IN PARAMETRIC DOWN CONVERSION

A. General conceptions in optical parametric down conversion:

Optical parametric down-conversion (OPDC) is a powerful tool for generating squeezed states. In OPDC, a beam of radiation, called the pump, is incident on a birefringent crystal (or a periodically poled crystal). The pump is intense enough so that nonlinear effects lead to the conversion of its photons into pairs of correlated photons, called signal and idler. In this paper, we call them signal and idler in both degenerate and non-degenerate cases. The down-conversion is said to be of type-I or type-II, depending on whether the photons in the pair have parallel or orthogonal polarization, or it is called quasi-phase matching (QPM), if the crystal is periodically poled crystal. The photons in pair may come out in different directions or in the same direction (collinearly), shown in FIG. 1.

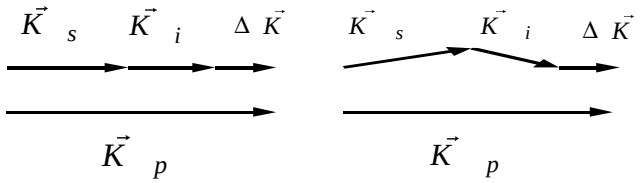

(a) (b)

FIG. 1. Phase matching condition. (a) collinear case. (b) non-collinear case

The frequency and direction of the photons is determined by phase matching conditions:

$$\omega_p = \omega_s + \omega_i, \qquad \vec{K}_p = \vec{K}_s + \vec{K}_i + \Delta\vec{K}. \tag{2.1}$$

The subscripts of p, s, and i indicate pump, signal and idler. ΔK is the wave number mismatch between the modes. When the phase matching condition is satisfied, ΔK is zero for birefringent phase matching; and it is equal to $2\pi/\Lambda$ for QPM case, where Λ is the grating period of the periodically poled crystal. The phase matching condition constrains emission in cones around the pump.

B. Basic equations and correlation functions in non-degenerate optical parametric oscillation

There are two situations for OPDC process: under threshold and above threshold, which are also called spontaneous parametric down-conversion (SPDC) and optical parametric down-conversion (OPDC) respectively. The quantum correlations exist in both cases. There are numerous theoretical analyses [14-17], interesting experiments [7,9,10,13,18-20], and several review papers [3,8,11] study SPDC. Interested readers could refer to those papers. SPDC deals with microscopic states of light, i.e., states in which the number of photons is low. It would be of great interest to study macroscopic squeezed states, namely laser like beams having non-classical statistics.

Here we give a review on the noise characteristics of the phase and intensity in a two-mode optical parametric oscillator (OPO) above threshold. The emphasis is on the transmitted spectrum of fluctuations in the difference between signal and idler quadrature amplitudes including the effect of phase diffusion in the signal and idler modes. One finds that the noise reduction is possible for particular choices of quadrature-phase amplitudes, which indicates a perfect quantum correlations of phase and intensity between the signal and idler.

In terms of the familiar photon annihilation and creation operators a and a^+ for a single-mode field of frequency ω_p, a pair of conjugate quadrature operators is given by Eq.(2.2), with commutation relation [X,Y]=2i and corresponding uncertainty product $\Delta X\, \Delta Y \geq 1$.

$$X = (a + a^+) \qquad\qquad Y = -i(a - a^+) \tag{2.2}$$

Light in a coherent state or in a vacuum state is in a minimal-uncertainty state with equal variance for each of the two quadrature components. Squeezed states may or may not be minimal-uncertainty states but are such that one quadrature component has variance less than 1. The fluctuations expressed by the uncertainty product can be graphically represented (shown in FIG. 2.) by a symmetric error circle for a coherent state (dashed line) while for a squeezed state this error circle is squeezed into an error ellipse (solid line). The quantity $V(\theta)$ is the phase dependence of the rms noise of the field $X(\theta)=X\cos(\theta)+Y\sin(\theta)$ as a function of θ for a squeezed state.

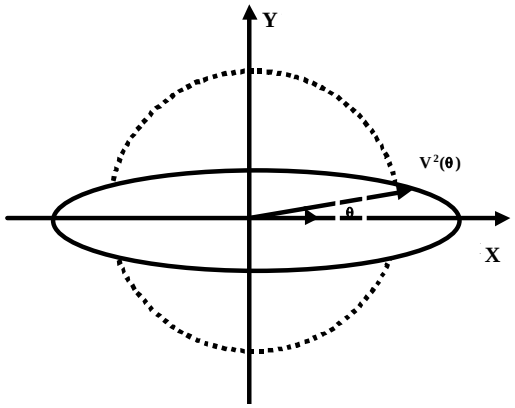

FIG. 2. Phase plot of the uncertainty in the quadrature amplitudes of the electric field

The simple theoretical model for this optical cavity is described as following. The pump, signal and idler fields are confined in an optical cavity. We assume perfect phase matching and neglect any loss other than the transmission through the coupling mirror. In a generalized P representation, one can establish a correspondence between stochastic amplitudes α_i (and α_i^+) and mode operators a_s, a_i and a_p, which are boson operators for the signal, idler and pump cavity modes. However, α_i and α_i^+ are on longer complex conjugates. That is α_i^+ is not equal to α_i^*.

The stochastic equations of motion for the field amplitudes α_i that describing the oscillation are [21]:

$$\begin{aligned}
\frac{d}{dt}\alpha_s &= -\kappa_s\alpha_s + g\alpha_p\alpha_i^+ + (g\alpha_p)^{1/2}\xi_s(t) \\
\frac{d}{dt}\alpha_i &= -\kappa_i\alpha_i + g\alpha_p\alpha_s^+ + (g\alpha_p)^{1/2}\xi_i(t) \\
\frac{d}{dt}\alpha_p &= -\kappa_p\alpha_p - g\alpha_s\alpha_i + E
\end{aligned} \tag{2.3}$$

together with the complex-conjugate equations. The first term of each equation is the cavity damping. We assume the signal and idler have the same damping rate $\kappa=\kappa_s=\kappa_i$. The second term describes the parametric coupling contribution, where g is the non-linear coupling constant, proportional to the second-order susceptibility of the

medium. The last term is the source term. In the equation of pump, E is the pump amplitude. In the equation of signal and idler, the $\xi_i(t)$ are δ correlated noise sources with zero mean and nonzero correlation, shown by Eq.(2.4),

$$\langle \xi_s(t)\xi_i(t')\rangle = \delta_{si}\delta(t-t'). \tag{2.4}$$

To study the behavior above threshold, we transform to phase and intensity variables in the vicinity of stationary states, defined as follows:

$$\begin{aligned} \delta I_{\pm} &= (I_s - I_s^0) \pm (I_i - I_i^0) \\ \delta I_p &= I_p - I_p^0, \delta\phi_+ = \phi_s + \phi_i \\ \delta\phi_p &= \phi_p, \phi_- = \phi_i - \phi_s \end{aligned} \tag{2.5}$$

where $I_i = \alpha^+_i \alpha_i$, $\varphi_i = \ln(\alpha^+_i/\alpha_i)/2i$, and I_i^0 and φ_i^0 are the steady-state deterministic solutions with $\varphi_p^0 = \varphi_s^0 + \varphi_i^0 = 0$. We consider the dynamics of small field fluctuations driven by the vacuum fluctuations entering the cavity through the coupling mirror. After linearization the equations of motion for $\delta I_{\pm}$, δI_p, $\delta\phi_+$, and $\delta\phi_p$ in the vicinity of the stationary state, we obtain the following equation for fluctuations [22]:

$$\begin{aligned} \frac{d}{dt}\delta I_+ &= 2g^2\left(\frac{I_0}{\kappa}\right)\delta I_p + F_+^0(t) \\ \frac{d}{dt}\delta I_p &= -\kappa_p \delta I_p - \kappa\delta I_+ \\ \frac{d}{dt}\delta I_- &= -2\kappa\delta I_- + F_-^0(t) \\ \frac{d}{dt}\delta\phi_+ &= -2\kappa\delta\phi_+ + 2\kappa\delta\phi_p + f_+^0(t) \\ \frac{d}{dt}\delta\phi_p &= -g^2\left(\frac{I^0}{\kappa}\right)\delta\phi_+ - \kappa_p\delta\phi_p \\ \frac{d}{dt}\phi_- &= f_-^0(t) \end{aligned} \tag{2.6}$$

where $I_s^0 = I_i^0 = I^0$ and $\delta I_{\pm}$, δI_p, $\delta\phi_+$, $\delta\phi_{3+}$, are the fluctuations of $I_{\pm}$, I_p, ϕ_+, ϕ_3, which are damping with stable points of zero, while the decoupled signal-idler phase difference ϕ_- undergoes a continuous diffusion.

The nonzero noise correlations are:

$$\begin{aligned} \left\langle F_+^0(t)F_+^0(t')\right\rangle &= -\left\langle F_-^0(t)F_-^0(t')\right\rangle = 4\kappa I^0\delta(t-t') \\ \left\langle f_-^0(t)\,f_-^0(t')\right\rangle &= -\left\langle f_+^0(t)\,f_+^0(t')\right\rangle = \left(\frac{\kappa}{I^0}\right)\delta(t-t') \end{aligned} \tag{2.7}$$

Stationary noise spectra for the field transmitted through a single port cavity are defined:

$$\begin{aligned} S_{ij} &= \int_{-\infty}^{\infty} e^{i\omega\tau}\left\langle \tilde{a}_i^+(t)\tilde{a}_j(t+\tau)\right\rangle d\tau \\ C_{ij} &= \int_{-\infty}^{\infty} e^{i\omega\tau}\left\langle \tilde{a}_i(t)\tilde{a}_j(t+\tau)\right\rangle d\tau \end{aligned} \tag{2.8}$$

The creation and annihilation operators in Eq. (2.8) denote the field external to the cavity, because we are interested in the fluctuations of the fields emitted by the cavity (not the fields inside the cavity). The algebra of this transform is given in [23]. These S_{ij} and C_{ij} are readily calculated, see [22]. The fluctuations in the signal-idler intensity difference δI_- and in phase sum $\delta\phi_+$ are negative in the P representation, implying noise levels below the vacuum or shot-noise limit [22, 23]. Since $\phi_s+\phi_i$ has minimal fluctuations, the signal and idler phases ϕ_s and ϕ_i are correlated. Also, I_s-I_i has minimal fluctuations, hence, the intensity fluctuations are correlated. These correlations exist both under threshold and above threshold [23].

Under the condition that intensity undergoes small stable fluctuations on a time scale much shorter than that of phase fluctuation occur, we expect to infer quadrature-phase information of the signal by measuring the quadrature phase of the idler given their quantum correlations. The quantity $V(\theta,\phi)$, the fluctuation spectrum in the signal and idler quadrature amplitude difference $X_s(\theta)$-$X_i(\phi)$, is a direct measure of the error in the inferring of the signal amplitude $X_s(t)$, given an experimental determination $X_i(t)$ of idler amplitude,

$$V(\theta,\phi)=\frac{1}{2}\left\langle[X_s(t)-X_i(t)]^2\right\rangle=1+2[\left\langle a_s^+a_s\right\rangle-\cos(\theta+\phi)\langle a_s a_i\rangle]. \tag{2.9}$$

Here, θ and ϕ are the phases of signal and idler, respectively. $V(\theta,\phi)$ is minimum for $\theta=-\phi$. When $V(\theta,\phi)=0$, it means that there is a perfect correlation between $X_s(t)$ and $X_i(t)$.

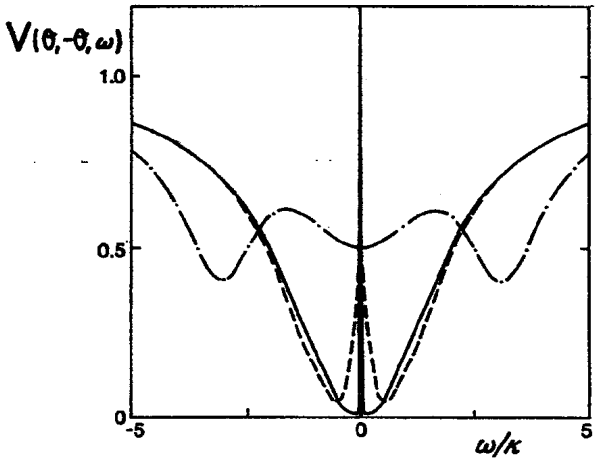

FIG. 3. Plot of $V(\theta,-\theta,\omega)$ as a function of ω/κ.Solid line is near threshold ($E/E_{th}=1.01,\kappa_p/\kappa=0.01$). Dash-dotted line is well above threshold with a good pump ($E/E_{th}=50,\kappa_p/\kappa=0.1$). Dashed line is well above threshold with an excellent pump ($E/E_{th}=20,\kappa_p/\kappa=0.01$) [15].

Figure 3 shows the spectrum of fluctuation in the signal and idler quadrature amplitude difference for various parameters. $V_{-\theta}$ indicates an EPR correlation. The coherent-noise spike for $E/E_{th} > 1$ at $\omega=0$ is due to the phase diffusion of ϕ_-, the decoupled signal-idler phase difference, which is the large but narrow Lorentzian proportional to $(1/2)((1/8I^0)^2+(\omega/\kappa)^2)^{-1}$. Near threshold (solid curve), phase and intensity fluctuations are suppressed near $\omega=0$, shown by the fact that $V(\theta,-\theta,\omega)\to 0$ near $\omega=0$.This is also true below threshold as $E/E_{th}\to 1$. Well above threshold with a good pump (dashed-doted curve), phase fluctuations are suppressed at higher frequency $\omega/\kappa\sim(2(\kappa_3/\kappa)(E/E_{th}))^{1/2}$. The two side peaks indicate nearly perfect suppression of phase fluctuation. The central dip

is the intensity fluctuation spectrum. Well above threshold with an excellent pump (dash curve), the bandwidth intensity fluctuation reduction extend to $\omega/\kappa \sim 2$, and perfect phase fluctuation reduction also occurs at higher frequency. The minimum uncertainty relation gives us 1 for two non-commuting observables, which determines the vacuum noise level. Thus the observation of $V(0,0)<0.5$ and $V(\pi/2,-\pi/2)<0.5$ indicate a squeezed state. We also notice that this EPR correlation effect occurs both above ($E/E_{th}<1$) and below threshold ($E/E_{th}<1$).

We know that for two non-commuting observables, for example P and Q with [P, Q]=2i, the minimum uncertainty relation is $\Delta P \Delta Q=1$, which determines the vacuum noise level. Notice in FIG. 3, $V(\theta,\phi)$ is less than 1 (less than vacuum noise level). The ability to infer either of the non-commuting signal observables with a precision below vacuum noise level is a direct example of an EPR correlation [24]. The noise reduction possible for particular choices of quadrature-phase amplitudes indicates a perfect correlation of both intensity and phase between signal and idler.

III. REVIEW OF EXPERIMENTS

A. Two-photon entanglement in type-II optical parametric down conversion (OPDC)

The nature of the two-photon state for type-II OPDC is such that it allows a number of interesting quantum-mechanical interference experiments, such as anti-correlation and quantum beating, to be performed. Those experiments illustrate the entanglement of spin and space-time (or in frequency and wave number) variables and the generation of EPR states.

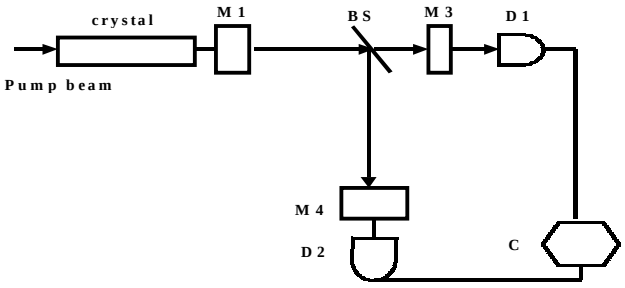

FIG. 4. The transformation of the beam by linear optical element.
BS is a 50-50 polarization-independent beam splitter

Here we consider collinear degenerate beams passing through a system like FIG. 4. The optical element M1 is one set of phase plate oriented so that its fast and slow axes are parallel to the o and e axes of the crystal. BS is a 50/50 polarization independent beam splitter. M3 and M4 are Glan-Thompson linear polarization analyzers, followed by a narrow bandwidth interference spectral filter. The polarization analyzers are oriented at 45° relative to o-ray and e-ray polarization planes of the crystal. The average coincidence counting rate is given by:

$$R_c = \lim_{T\to\infty} \frac{1}{T} \int_0^T dT_1 \int_0^T dT_2 \left\langle \Psi \mid E_1^- E_2^- E_2^+ E_1^+ \mid \Psi \right\rangle \times S(T_1 - T_2) \tag{3.1}$$

where the electric fields are defined in free space. The subscripts j=1,2 means that the fields is evaluated at the detector j at time T_j. S(t) is the coincidence window function, which is defined so that S=1 for $|t|<t_{coin}$ and goes to zero rapidly for $|t|>t_{coin}$. With state $|\psi>$ in a linear superposition of the vacuum state and a state containing two photons, it is easy to see that [8]:

$$\left\langle \Psi \mid E_1^- E_2^- E_2^+ E_1^+ \mid \Psi \right\rangle = \left| \left\langle 0 \mid E_2^+ E_1^+ \mid \Psi \right\rangle \right|^2 = \left| A(t_1, t_2) \right|^2 \tag{3.2}$$

where the function $A(t_1, t_2)$ is referred to as the two-photon amplitude.

The experimental coincidence counting rate depends on the optical path difference between the two arms is shown in FIG. 4. When the delay is zero, it shows two-photon anti-correlation in FIG. 5.

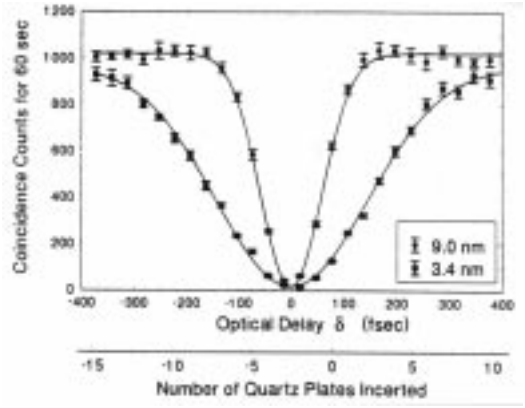

FIG. 5. The coincidence counting rate for two set of filters with FWHM of 3.4 and 9.0 nm.
The solid curves are Gaussian fits[7].

The "anti-correlation" is the result of the quantum superposition (cancellation) of the two-photon probability amplitudes |o-ray transmitted to D1>⊗|e-ray reflected to D2> and |e-ray transmitted to D1>⊗|o-ray reflected to D2>, when the orthogonal polarized photon pairs is incident through a single port of the beam splitter [7]. This phenomenon is a typical quantum two-photon interference effect, even though there's no interferometer involved. More classical two-photon quantum interference experiments and theoretical analysis refer to [18,14].

We now consider collinear non-degenerate beams passing through a system like FIG. 4, M1 is a set of phase plate oriented parallel to the o and e axes. M3 and M4 are linear analyzers followed by a filter centered at λ_1 and λ_2, respectively. The analyzers in front of the detectors are oriented at angle of 45° relative to the o axis. The width of the filters are chosen so that the overlap of their spectral ranges is negligible; therefore, we may assume that only one wavelength reaches each detector. The formulas of two-photon amplitude and coincident counting rate are given by Eq. (3.3) [8]:

$$R_c \approx R_0 \sin^2\left[\frac{\omega_d(\tau - \tau_0)}{2}\right] \tag{3.3}$$

where $\omega_d=2\pi c(1/\lambda_1-1/\lambda_2)$ and τ_0 is the average of the time difference it takes o-ray and e-ray wave packets to cross the crystal.

In a simplified picture, we have, for the wave function just before it enters the beam splitter. The state generating the amplitude is entangled jointly in polarization and wavelength given by Eq. (3.4):

$$\Psi = e^{i\omega_d(\tau-\tau_0)/2}\left|\lambda_1, o\right\rangle\left|\lambda_2, e\right\rangle + e^{-i\omega_d(\tau-\tau_0)/2}\left|\lambda_1, e\right\rangle\left|\lambda_2, o\right\rangle \tag{3.4}$$

This joint entanglement is crucial to the interference between the two amplitudes. The experimental result is shown in FIG. 6. Single-detector counting rate shows no modulation when either the polarization in front of the detector is rotated or there is a change in the relative time delay of the two polarization beams. This is shown in the upper part of FIG. 6. If we keep the delay fix and vary the orientation of the polarizers, then we get the interference effects – quantum beat similar to the examples of changing optical path difference [7,18].

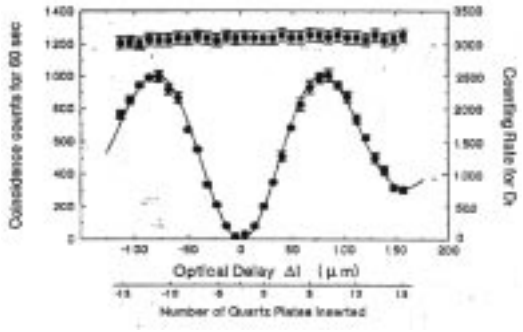

FIG. 6. Difference frequency oscillations with 100% visibility showing the two-photon quantum beats between orthogonal polarized photons [25].

It demonstrates both space-time and spin entanglement in this single experiment. The space-time entanglement is illustrated by the beating at different frequency. The polarization effect is observed by rotating the analyzers in front of those detectors. In fact when the polarizers are at 45°, it corresponds to the EPR entangled states, which is shown by the cancellation amplitude [8].

B. Squeezed states generated in degenerate parametric down conversion (DPDC)

Kimble and his co-workers [26] use the method of DPDC generate squeezed states, which showed the noise reductions greater than 50% relative to the vacuum noise level in a balanced homodyne detector (further increased to 75% in a DOPO [27]).

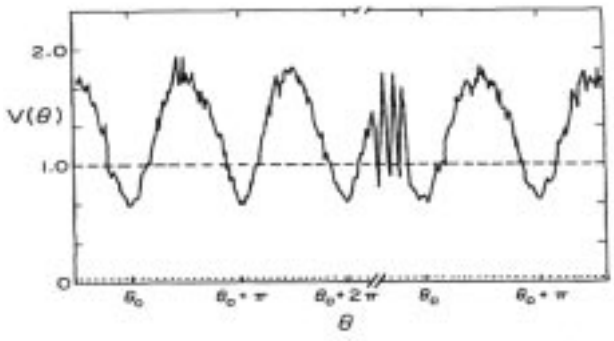

FIG. 7.Measurement of the phase dependence of rms noise voltage V(θ) from a balanced homodyne detectors displayed as a function of local oscillator phase at fixed frequency and bandwidth [26].

The observation of squeezing of the signal beam centers on an analysis of the spectral distribution of fluctuations of the signal formed by the subtraction of the two photo-currents produced by photo-diodes. FIG. 7. shows the phase dependence of the rms noise voltage V(θ) from the balanced homodyne receiver as a function of local oscillator phase θ at fixed analysis frequency. The dashed line corresponds to the noise level V_0 set by vacuum fluctuations. Values of V(θ) below the dashed lines in FIG. 7. represent observations of squeezing of the signal field.

In order to make a quantitative comparison of the results with theoretical predictions, the relationship between the detected external fields and the intracavity field of the OPO needs to be considered. The spectrum of squeezing S(θ,ω) of the output field assuming an ideal single-port cavity is given in FIG. 8. If the cavity is not a single-port device, the observable phase-dependent variations in the amplitude of the output field are degraded by the factor of $(1+g)^{-1}$. g is the ratio of all other loss rate other than through the output coupler to the loss rate through the output coupler.

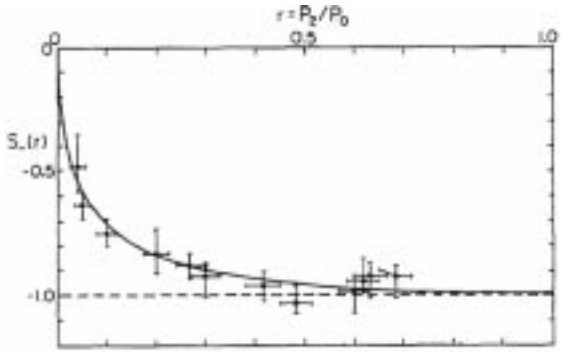

FIG. 8. Comparison of the experimental measurement and theoretical prediction (solid curve) of the spectrum of squeezing $S_-(r = E/E_{th})$. Perfect squeezing occurs for $S_-(r)=-1$ and is indicated by the dashed line [26].

The spectrum of squeezing extracted from the measurement (FIG. 8.) indicates that the observed squeezing resulted from a field squeezed more than tenfold [26].

IV. SUMMARY

This paper gives a review of the correlations between photon pairs generated by parametric down conversion. The analysis of non-degenerate OPO above threshold gives the result that the phase and intensity of the two photons are correlated. Noise reduction in phase and intensity can be achieved by particular choice of quadrature phase amplitudes. Since the sum of the two photons' phase ($\varphi_s+\varphi_i$) and the difference of the intensity (I_S-I_i) have minimal fluctuations, the two photons are in entangled states. Just like the EPR states, the measurement of an observable of either particle determines the value of that observable of the other particle. Several experiments of squeezed states generated via parametric down conversion with either squeezed spectrum or squeezed intensity. These showed that PDC is a powerful tool to generate squeezed states. The properties of squeezed state and correlations can be used to reduce quantum noise.

REFERENCE:

[1] L. Hardy, Phys. Rev. Lett. A 161, 326 (1992)

[2] A. A. Malygin, A. N. Penin, and A. V. Sergienko, Dokl. Akad. Nauk SSSP 281, 308 (1985)

[3] M. H. Rubin, Phys. Rev. A 54, 5349 (1996)

[4] T. B. Pittman, Y. H. Shil, D. V. Strekalov, and A. V. Sergienko, Phys. Rev. A 52, R3429 (1995)

[5] T. B. Pittman, D.V. Strekalov, D. N. Klyshko, M. H. Rubin, A. V. Sergienko and Y. H. Shih, Phys. Rev. A 53, 2804 (1996)

[6] T. P. Grayson and G. A. Barbosa, Phys. Rev. A 49, 2948 (1994)

[7] Y. H. Shih and A. V. Sergienko, Phys. Lett. A 186, 29 (1994)

[8] M. H. Rubin, D. N. Klyshko, Y. H. Shih, and A. V. Sergienko, Phys. Rev. A 50, 5122 (1994)

[9] P. R. Tapster, J. G. Rarity, and J. S. Satchell, Phys. Rev. A 37, 2963 (1988)

[10] Y. H. Shih and C. O. Alley, Phys. Rev. Lett. 61, 2921 (1988)

[11] J. P. Dowling, Phys. Rev. A 57, 4736 (1998)

[12] X. Y. Zou, L. J. Wang and L. Mandel, Opt. Comm. 84, 351 (1991)

[13] P. R. Tapster, S. F. Seward, and J. G. Rarity, Phys. Rev. A 44, 3266 (1991)

[14] R. Ghosh, C. K. Hong, Z. Y. Ou and L. Mandel, Phys. Rev. A 34, 3962 (1986)

[15] S. Friberg, C. K. Hong and L. Mandel, Opt. Comm. 54, 311 (1985)

[16] X. T. Zou and L. Mandel, Phys. Rev. A 41, 475 (1990)

[17] C. K. Hong and L. Mandel, Phys. Rev. A 31, 2409 (1985)

[18] C. K. Hong, Z. Y. Ou and L. Mandel, Phys. Rev. Lett. 59, 2044 (1987)

[19] Z. Y. Ou and L. Mandel, Phys. Rev. Lett. 62, 2941 (1989)

[20] Z. Y. Ou and L. Mandel, Phys. Rev. Lett. 61, 54 (1988)

[21] K. J. McNeil and C. W. Gardiner, Phys. Rev. A 28, 1560 (1983)

[22] M. D. Reid and P. D. Drummond, Phys. Rev. Lett. 60, 2731 (1988)

[23] S. Reynaud, C. Fabre, and E. Giacobino, J. Opt. Soc. Am. B4, 1520 (1987)

[24] A. Einstein, B. Podolsky, and N. Rosen, Phys. Rev. 47, 777 (1935)

[25] Y. H. Shih and A. V. Sergienko, Phys. Rev. A 50, 2564 (1994)

[26] L. A. Wu, H. J. Kimble, J. L. Hall, and H. F. Wu, Phys. Rev. Lett. 57, 2520 (1986)

[27] S. Z. Jin and M. Xiao, Phys. Rev. A 49, 499 (1994)